

White matter lesions

Spatial heterogeneity, links to risk factors, cognition, genetics, and atrophy

Mohamad Habes, PhD, Aristeidis Sotiras, PhD, Guray Erus, PhD, Jon B. Toledo, MD, Deborah Janowitz, MD, David A. Wolk, MD, Haochang Shou, PhD, Nick R. Bryan, MD, Jimit Doshi, MSc, Henry Völzke, MD, Ulf Schminke, MD, Wolfgang Hoffmann, MD, MPH, Susan M. Resnick, PhD,† Hans J. Grabe, MD,‡ and Christos Davatzikos, PhD‡

Correspondence

Dr. Habes
habesm@uphs.upenn.edu

Neurology® 2018;91:e964-e975. doi:10.1212/WNL.00000000000006116

Abstract

Objectives

To investigate spatial heterogeneity of white matter lesions or hyperintensities (WMH).

Methods

MRI scans of 1,836 participants (median age 52.2 ± 13.16 years) encompassing a wide age range (22–84 years) from the cross-sectional Study of Health in Pomerania (Germany) were included as discovery set identifying spatially distinct components of WMH using a structural covariance approach. Scans of 307 participants (median age 73.8 ± 10.2 years, with 747 observations) from the Baltimore Longitudinal Study of Aging (United States) were included to examine differences in longitudinal progression of these components. The associations of these components with vascular risk factors, cortical atrophy, Alzheimer disease (AD) genetics, and cognition were then investigated using linear regression.

Results

WMH were found to occur nonuniformly, with higher frequency within spatially heterogeneous patterns encoded by 4 components, which were consistent with common categorizations of deep and periventricular WMH, while further dividing the latter into posterior, frontal, and dorsal components. Temporal trends of the components differed both cross-sectionally and longitudinally. Frontal periventricular WMH were most distinctive as they appeared in the fifth decade of life, whereas the other components appeared later in life during the sixth decade. Furthermore, frontal WMH were associated with systolic blood pressure and with pronounced atrophy including AD-related regions. AD polygenic risk score was associated with the dorsal periventricular component in the elderly. Cognitive decline was associated with the dorsal component.

Conclusions

These results support the hypothesis that the appearance of WMH follows age and disease-dependent regional distribution patterns, potentially influenced by differential underlying pathophysiologic mechanisms, and possibly with a differential link to vascular and neurodegenerative changes.

†These authors contributed equally to this work.

From the Center for Biomedical Image Computing and Analytics (M.H., A.S., G.E., N.R.B., J.D., C.D.), Department of Neurology and Penn Memory Center (M.H., D.A.W.), and Department of Biostatistics and Epidemiology (H.S.), University of Pennsylvania, Philadelphia; Department of Psychiatry (M.H., D.J., H.J.G.), Institute for Community Medicine (M.H., H.V., W.H.), and Department of Neurology (U.S.), University of Greifswald, Germany; Department of Neurology (J.B.T.), Houston Methodist Hospital, TX; German Center for Neurodegenerative Diseases (W.H., H.J.G.), Rostock/Greifswald, Germany; and Laboratory of Behavioral Neuroscience (S.M.R.), National Institute on Aging, Baltimore, MD.

Go to Neurology.org/N for full disclosures. Funding information and disclosures deemed relevant by the authors, if any, are provided at the end of the article.

Glossary

AD = Alzheimer disease; **BLSA** = Baltimore Longitudinal Study of Aging; **deep** = deep white matter; **dors.** = dorsal periventricular; **fron.** = frontal periventricular; **post.** = posterior periventricular; **SHIP** = Study of Health in Pomerania; **WMH** = white matter hyperintensities; **WMHC** = white matter hyperintensities component.

White matter lesions or hyperintensities (WMH) are common findings in older adults, characterized by a hyperintense signal on T2-weighted MRIs. WMH are considered a type of sporadic small vessel disease¹ and are associated with gray matter atrophy in Alzheimer disease (AD)-related regions,^{2,3} cognitive decline, and increased risk of dementia.⁴ WMH have therefore received increasing attention as a contributor to brain aging, neurodegeneration, and dementia. In addition, there is mounting evidence that the spatial location of WMH may have distinct neuropathologic and clinical associations.^{5–11}

Despite evidence indicating differential etiology of location of WMH and increased likelihood of dementia depending on the spatial distribution,¹² most studies measure total WMH burden. Only a few studies have considered differential region-specific WMH associations^{7,11,13–15}; however, such studies use empirically defined WMH categories. Therefore, we compute data-driven WMH definitions, by modeling inherent WMH covariation patterns in the MRIs,¹⁶ via nonnegative matrix factorization.^{17,18} We tested the hypothesis that WMH occurrence exhibits spatial heterogeneity, rather than simply being a process of uniformly increasing volume of abnormal-appearing tissue. We aimed to deepen our understanding of the spatial heterogeneity of WMH and their progression with age, as well as to investigate their correlates with clinical and genetic risk factors, brain atrophy, and cognitive decline.

Methods

Study of Health in Pomerania participants

We included 1,836 participants encompassing a wide age range (22–84 years) from the Study of Health in Pomerania (SHIP) cohort, led by the Institute for Community Medicine at the University Medicine Greifswald, Germany. The SHIP project consists of 2 independent cohorts, SHIP-2 and SHIP-TREND. SHIP participants were recruited using a 2-stage stratified and cluster sampling scheme to represent a sample between 20 and 79 years. First, regional communities were selected; second, residence registries were used to draw a random representative sample. Characteristics of the included and excluded samples are provided in table 1. An outline of the exclusion criteria is presented in the online data available from Dryad (figure e-1, doi.org/10.5061/dryad.k6k42cq).

Data assessment and laboratory work in SHIP¹⁹ were described previously in more detail by Habes et al.^{3,20} and are presented in the online data available from Dryad (section e-1, doi.org/10.5061/dryad.k6k42cq). In our analysis, we included the following variables: (1) smoking, (2) education,

(3) systolic blood pressure, (4) glycosylated hemoglobin, (5) waist circumference, (6) antihypertensive medication use, (7) antidiabetic medication use, (8) lipid-lowering medication use, (9) total cholesterol, (10) low-density lipoprotein, (11) high-density lipoprotein, (12) intima-media thickness (available for n = 1,817), and (13) AD polygenic risk score (available for n = 985), which was calculated as described in data available from Dryad (section e-2). Determination of participants with possible cognitive impairment in SHIP has been described in data available from Dryad (section e-3).

Baltimore Longitudinal Study of Aging participants

The Baltimore Longitudinal Study of Aging (BLSA) is a long-running study of aging led by the National Institute on Aging in Baltimore, MD. BLSA participants are a volunteer sample of community-dwelling individuals. Specific recruitment strategies have varied over time, but all participants meet health criteria at entry. The neuroimaging substudy of the BLSA has been described previously.²¹ We included in this study 307 cognitively normal and mild cognitive impairment participants with 747 observations to examine longitudinal associations with cognition in an independent aging cohort. Participants of the BLSA have received MRI and cognitive testing at the same visit. Every participant had at least 2 observations of WMH and complete cognition information, including diagnostic designation based on cognitive status. Table 2 presents the characteristics of BLSA at baseline. We included the following neuropsychological scores for the BLSA sample: (1) the Benton Visual Retention Test for visual memory assessment; (2) Trail Making Test, Parts A and B, assessing attention and executive function, respectively; and (3) the California Verbal Learning Test.

Standard protocol approvals, registrations, and patient consents

The ethics committee of the Medical Faculty of the University of Greifswald approved the SHIP study. All participants provided written informed consent. The National Institute of Environmental Health Sciences institutional review board approved the BLSA protocol, and written informed consent was obtained at each study visit.

Image acquisition and preprocessing

Imaging parameters were described by Hegenscheid et al.²² for SHIP and by Venkatraman et al.²³ for BLSA; additional details are given in data available from Dryad (section e-4, doi.org/10.5061/dryad.k6k42cq). Image analysis was performed using T1-weighted and fluid-attenuated inversion recovery brain MRIs, described in more detail in data available from Dryad (section e-5). Briefly, an automated multimodal

Table 1 Characteristics of the SHIP sample

Characteristic	SHIP subcohort		SHIP sample included (n = 1,836)	SHIP sample excluded (n = 1,230)
	SHIP-2 (n = 577)	SHIP-TREND (n = 1,259)		
Age, median (SD), y	55.0 (11.8)	51.1 (13.6)	52.2 (13.16)	55.7 (14.5)
Sex, n (%), female	316 (54.78)	719 (57.1)	1,035 (56.4)	559 (45.5)
Systolic blood pressure, median (SD), mm Hg	130.0 (17.7)	124.5 (17.1)	126.0 (17.4)	130.0 (18.4)
Glycosylated hemoglobin (HbA _{1c}), median (SD), %	5.3 (0.8)	5.2 (0.6)	5.2 (0.7)	5.3 (0.8)
Total cholesterol, median (SD), mmol × L ⁻¹	5.5 (1.1)	5.5 (1.1)	5.5 (1.1)	5.4 (1.1)
High-density lipoprotein, median (SD), mmol × L ⁻¹	1.4 (0.4)	1.4 (0.4)	1.4 (0.4)	1.40 (0.4)
Low-density lipoprotein, median (SD), mmol × L ⁻¹	3.4 (0.9)	3.4 (0.9)	3.4 (0.9)	3.3 (0.9)
Waist circumference, median (SD), cm	89.5 (12.7)	88.0 (12.6)	88.3 (12.6)	91.0 (13.2)
Mean intima-media thickness, median (SD), mm	1.2 (0.3) ^a	1.1 (0.3) ^b	1.2 (0.3) ^c	1.2 (0.3) ^d
Cigarette smoking, n (%)				
Never-smoker	232 (40.2)	520 (41.3)	752 (41.0)	466 (37.9)
Ex-smoker	225 (39.0)	427 (33.9)	652 (35.5)	510 (41.4)
Current smoker	120 (20.78)	312 (24.8)	432 (23.5)	254 (20.7)
Medication				
Antidiabetics, n (%)	27 (4.7)	39 (3.01)	66 (3.6)	80 (6.5)
Antihypertensive, n (%)	214 (37.1)	382 (30.3)	596 (32.5)	464 (37.7)
Lipid-lowering drugs, n (%)	80 (13.9)	100 (7.9)	180 (9.8)	180 (14.6)
Education, n (%)				
<8 y	98 (17.9)	165 (13.1)	263 (14.3)	268 (21.7)
8–10 y	339 (58.7)	706 (56.1)	1,045 (56.9)	637 (51.7)
>10 y	140 (24.23)	388 (30.8)	528 (28.8)	325 (26.4)
Physical activity, n (%)				
No	162 (28.1)	398 (31.6)	560 (30.5)	443 (36.0)
>0–1 h/wk	90 (15.6)	199 (15.8)	289 (15.7)	169 (13.7)
>1–2 h/wk	169 (29.3)	356 (28.3)	525 (28.6)	318 (25.9)
>2 h/wk	156 (27.0)	306 (24.3)	462 (25.2)	300 (24.3)

Abbreviation: SHIP = Study of Health in Pomerania.

^a Measure was available for 567.

^b Available for 1,250.

^c Available for 1,817.

^d Available for 1,210.

method was used to segment WMH, which were then aligned to a common template space. Structural T1-weighted MRIs for SHIP were processed using the protocols of the ENIGMA (Enhancing Neuro Imaging Genetics Through Meta Analysis) consortium for the calculation of cortical thickness (data available from Dryad, section e-5).

Identifying covariance components

WMH components (WMHCs) were identified using a non-negative matrix factorization method, which summarizes

complex multivariate patterns of covariation in the data with a predefined number of nonnegative components¹⁷ (data available from Dryad, section e-6, doi.org/10.5061/dryad.k6k42cq). The method was applied to the whole SHIP sample (n = 1,836) to derive a set of WMHCs. Participant-specific coefficients for each component were then calculated for both the SHIP and the BLSA cohorts to quantify corresponding WMH burden within each component.

Table 2 Characteristics of the BLSA sample

Characteristic	BLSA participants with 2 time points (n = 307)	BLSA participants with 3 time points (n = 101)	BLSA participants with 4 time points (n = 21)	BLSA participants with 5 time points (n = 8)
Age, median (SD), y	73.8 (10.2)	78.7 (8.2)	82.8 (3.2)	83.3 (2.3)
Follow-up time, median (SD), y	2.5 (1.2)	4 (0.9)	4.4 (0.9)	5.1 (0.4)
Sex, n (%), female	166 (53.9)	59 (58.4)	11 (52.3)	4 (50.0)
Education, median (SD), y	18.0 (2.4)	18.0 (2.1)	18.0 (2.2)	18.0 (2.5)
Cognitive scores, median (SD)				
Trail Making Test, Part A	30.0 (12.0)	30.0 (10.3)	30.0 (5.8)	30.5 (7.1)
Trail Making Test, Part B	71.0 (36.3)	75.0 (35.7)	70.0 (20.9)	73.0 (23.8)
Benton Visual Retention Test, total error score	6.0 (4.3)	7.0 (4.1)	6.0 (4.0)	6.0 (4.7)
California Verbal Learning Test, long-delay free recall	12 (3.3)	11.0 (3.4)	12.0 (3.3)	13.0 (3.9)
California Verbal Learning Test, short-delay free recall	11.0 (3.5)	11.0 (3.7)	12.0 (3.4)	12.0 (3.6)

Abbreviation: BLSA = Baltimore Longitudinal Study of Aging.

Note that higher scores for the Trail Making Tests and the Benton Visual Retention Test mean worse performance.

Statistical analysis

More details on the statistical analysis can be found in data available from Dryad (section e-7, doi.org/10.5061/dryad.k6k42cq). We examined relationships of the identified components with age in SHIP using linear regression models independently for each component, with age categorized in decades. In SHIP, cross-sectional WMHC trend lines were computed independently for each component using a linear regression model that included age and age² as predictors. For longitudinal temporal trends in BLSA, we used linear mixed-effects models with similar predictors. Significance of the differences between trend lines was assessed through permutation testing (data available from Dryad, section e-8). To assess possible staging of the WMH progression, we estimated a model of regional WMH progression based on the frequency of regional WMH presence across participants, similar to the method by Grothe et al.²⁴ In this analysis, each WMHC for each participant was categorized as WMH “present” or “absent,” according to a fixed threshold estimated from the total WMH volume for the complete sample.

We performed vertex-wise analysis of the cortical thickness in SHIP (n = 1,836) to inspect the relationship to each component. Results were considered significant if they survived cluster-wise correction for multiple comparisons at $p < 0.05$. We assessed the cross-sectional association between risk factors and WMHCs in the whole SHIP sample (n = 1,836) using a linear regression model for each component as outcome (resulting in 4 models). Similarly, we investigated cross-sectional associations of the 4 WMHCs with the AD polygenic risk score in the whole SHIP sample with available genotyping (n = 985) and in those older than 65 years (n = 189). All regression models using the whole age range SHIP sample were adjusted for age, age², sex,

education, and SHIP subcohort.²⁵ Models were Bonferroni-corrected by factor 4. Finally, we used independent linear mixed-effect models to investigate associations of longitudinal change in WMHCs with cognitive scores as outcome and WMHCs as predictors (one model at a time, resulting in 16 models) in BLSA (n = 307 and 747 observations). All models were adjusted for age, age², sex, educational level, and scanner type. Random slopes with age effect were included in the models in addition to random intercepts. Models were Bonferroni-corrected by factor 16. In all models, we applied a cubic root transformation on the WMHC values to normalize their distribution. Results were considered statistically significant if the 2-sided p value was <0.05 after Bonferroni correction. Analyses were performed using R software version 3.1.²⁶

Data availability

Data from SHIP are available after data application and signature of a data transfer agreement. The data dictionary and the online application form are available at: fvc.med.uni-greifswald.de/dd_service/data_use_intro.php. Involving a local collaborative partner to facilitate the application process is recommended.

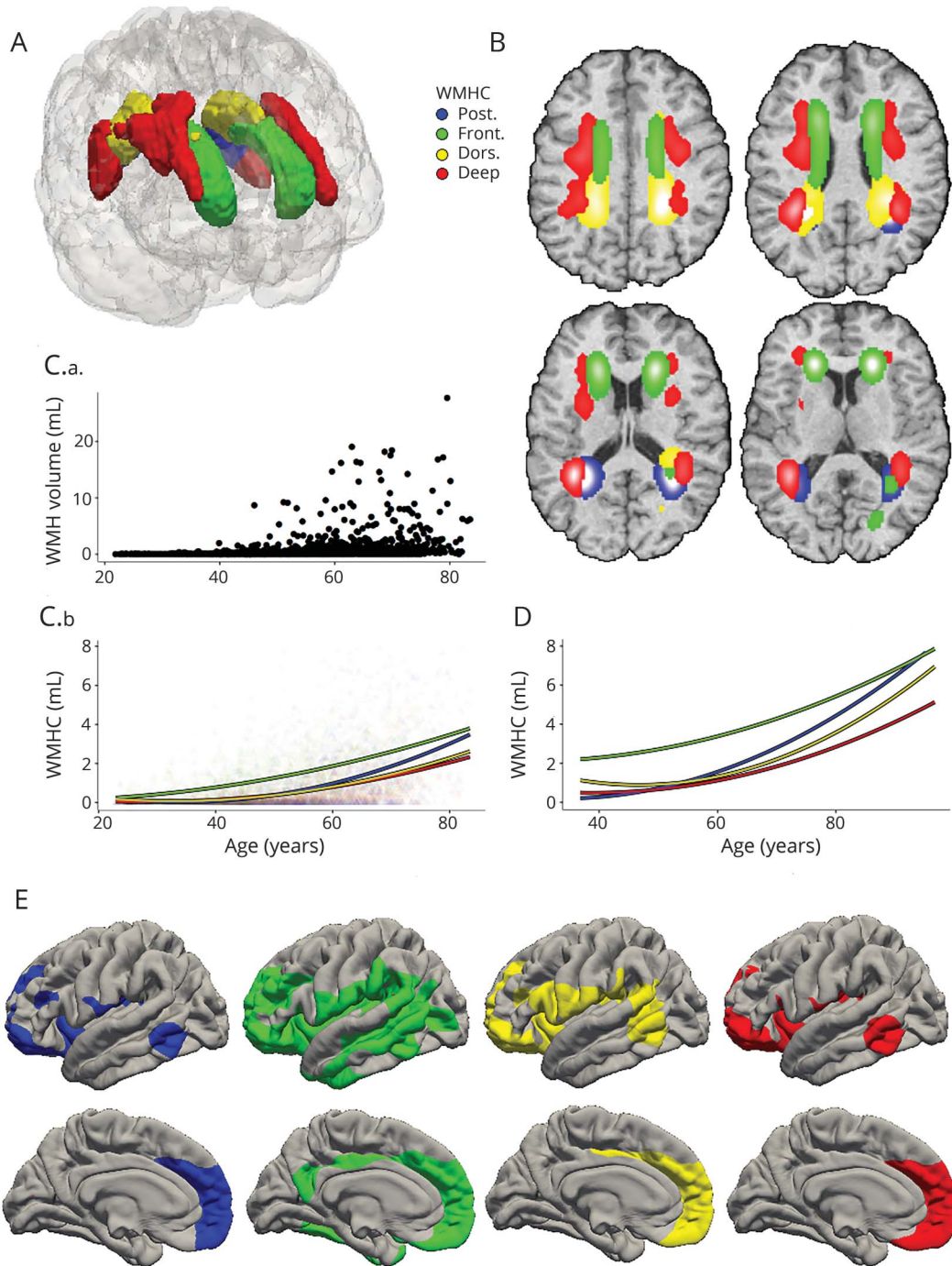
Data from the BLSA are available on request from the BLSA website (blsa.nih.gov). All requests are reviewed by the BLSA Data Sharing Proposal Review Committee and are also subject to approval from the NIH institutional review board.

Results

Spatial distribution of WMH covariance components

In the SHIP sample (n = 1,836), we identified 4 WMH covariance components (figure 1, A and B), selected according

Figure 1 Cross-sectional and longitudinal trend lines of WMHCs representing regional covariation



(A) Three-dimensional rendering of the 4 WMHCs calculated from the whole SHIP sample ($n = 1,836$). The 4 WMHCs are posterior periventricular (WMHC-post, blue), frontal periventricular (WMHC-fron., green), dorsal periventricular (WMHC-dors., yellow), and deep white matter (WMHC-deep, red). (B) Axial sections of the 4 WMHCs. (C.a) Total white matter hyperintensity volume as a function of age in the SHIP sample ($n = 1,836$). (C.b) Trend lines of the 4 WMHCs as a function of age for SHIP participants. (D) Longitudinal age trajectories of the 4 WMHCs in the Baltimore Longitudinal Study of Aging sample ($n = 307$ and 747 observations). (E) Cortical thickness reduction associated with the 4 WMHCs in SHIP ($n = 1,836$) after adjusting for age, age², sex, and SHIP subcohort. Results survived cluster-wise correction for multiple comparisons, $p < 0.05$. SHIP = Study of Health in Pomerania; WMHC = white matter hyperintensities component.

to previously defined criteria (data available from Dryad, section e-6 and figure e-2, doi.org/10.5061/dryad.k6k42cq). The robustness of the final components was validated through reproducibility experiments using random half-splits of the SHIP sample with similar age and sex distributions (data

available from Dryad, section e-6 and figure e-3). We quantified the extent to which these components were overlapping between the 2 splits by calculating the inner product of matching component pairs (data available from Dryad, table e-1). The median overlap value was 88%, showing highly

reproducible results. From the 4 components, the first 3 surrounded the ventricles and specified as periventricular posterior (WMHC-post, blue in figure 1), periventricular frontal (WMHC-fron., green in figure 1), and periventricular dorsal (WMHC-dors., yellow in figure 1) regions. The fourth component included the deep WMH and was located laterally to the other 3 components (WMHC-deep, red in figure 1). We applied the structural covariance approach on the BLSA baseline sample (n = 307) to assess the sensitivity of the approach toward different population characteristics (data available from Dryad, figure e-4). The median overlap value between components derived from SHIP vs BLSA was 66%, with the highest overlap in the frontal WMHC (data available from Dryad, table e-2).

Associations with age

We examined relationships of the identified components with age. Table 3 shows the differential association of WMHC-fron. with age in SHIP, as it was present from fifth decade of life, while other components were present from the sixth decade. Cross-sectional and longitudinal temporal trends of the 4 WMHCs are shown in figure 1, C and D. Supplementary analysis using permutation tests showed that the components had differential trend lines except between the WMHC-dors. and WMHC-deep components cross-sectionally (data available from Dryad, section e-7 and table e-3, doi.org/10.5061/dryad.k6k42cq). Figure 2 shows some hierarchical nesting across participants, both in SHIP and BLSA, as well as participants with distribution profiles that do not conform to the model, particularly in SHIP (approximately 10%) (more details in data available from Dryad, section e-9).

Associations with cortical thickness

We found widespread regional cortical atrophy associations in SHIP for all 4 WMHCs (n = 1,836, figure 1E). Gray matter decrease in the frontal, inferior parietal, and temporal cortex was more pronounced in association with the WMHC-fron. compared to the other components (data available from Dryad, section e-10, doi.org/10.5061/dryad.k6k42cq). We quantified the overlap in cortical atrophy regions associated with each of the 4 WMHCs. The amount of overlap between 2 regions is measured using their Dice coefficient (data available from Dryad, table e-4).

Associations with vascular risk factors, AD polygenic risk score, and cognition

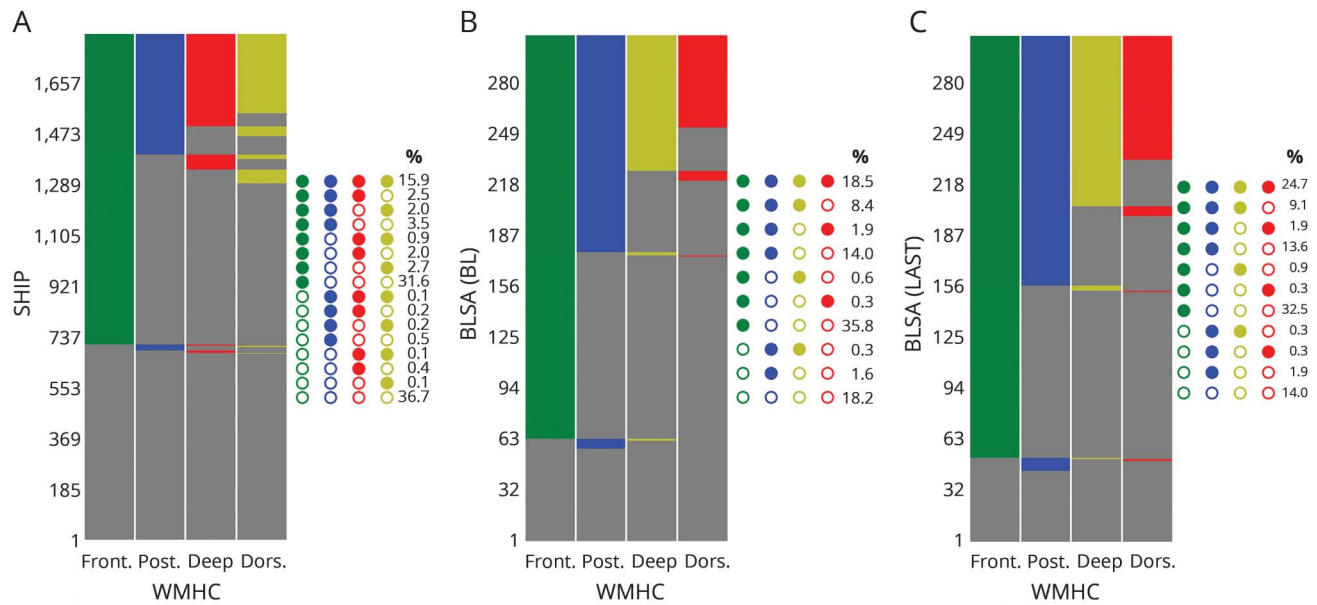
We found significant cross-sectional associations of WMHCs with vascular risk factors in the SHIP sample (n = 1,836, table 4). Specifically, intima-media thickness was significantly associated with WMHC-dors.; smoking was associated with the same component, in addition to WMHC-post. and WMHC-deep; higher blood pressure was associated with WMHC-fron.; and female sex was associated with more WMHC-fron. After exclusion of individuals with possible cognitive impairment (n = 178), only the associations of WMHC-fron. with higher blood pressure and WMHC-post. with smoking

Table 3 Linear regression models showing the association between the 4 WMHCs and age categorized in decades in SHIP

Age, y	WMHC-post.		WMHC-fron.		WMHC-dors.		WMHC-deep	
	Estimate (SE)	p Value (Bonferroni-corrected)	Estimate (SE)	p Value (Bonferroni-corrected)	Estimate (SE)	p Value (Bonferroni-corrected)	Estimate (SE)	p Value (Bonferroni-corrected)
>30-40 (n = 242)	0.070 (0.150)	1.000	0.235 (0.130)	1.000	0.170 (0.117)	1.000	0.055 (0.104)	1.000
>40-50 (n = 480)	0.124 (0.143)	1.000	0.554 (0.124)	<0.001 ^a	0.132 (0.111)	1.000	0.125 (0.099)	1.000
>50-60 (n = 464)	0.425 (0.153)	0.020 ^a	0.965 (0.132)	<0.001 ^a	0.355 (0.120)	0.012 ^a	0.378 (0.107)	0.002 ^a
>60-70 (n = 381)	1.049 (0.170)	<0.001 ^a	1.421 (0.147)	<0.001 ^a	0.761 (0.132)	<0.001 ^a	0.730 (0.118)	<0.001 ^a
>70 (n = 167)	1.957 (0.198)	<0.001 ^a	2.109 (0.170)	<0.001 ^a	1.403 (0.154)	<0.001 ^a	1.190 (0.137)	<0.001 ^a

Abbreviations: deep = deep white matter; dors. = dorsal periventricular; fron. = frontal periventricular; post. = posterior periventricular; SHIP = Study of Health in Pomerania; WMHC = white matter hyperintensities component. The models were adjusted for sex, smoking, education, systolic blood pressure, glycosylated hemoglobin, waist circumference, antihypertensive medication use, antidiabetic medication use, lipid-lowering medication use, total cholesterol, low-density lipoprotein, high-density lipoprotein, intima-media thickness, and SHIP substudy cohort.
^a Significance at level $p < 0.05$.

Figure 2 Heterogeneity and staging of WMH in the 4 WMHCs for (A) SHIP (n = 1,836), (B) BLSA baseline (n = 307), and (C) BLSA last MRI visit samples



Each row of the matrix corresponds to a study participant and each column to 1 of the 4 components. WMHC values were binarized (absence or presence of WMH) using a threshold value calculated as the median of total WMH volume for the baseline sample divided by 4. Absence of WMH is denoted by gray and presence by the indicative color of a component. The data tables show percentage of participants for different combinations of WMH presence in the 4 components. BL = baseline; BLSA = Baltimore Longitudinal Study of Aging; deep = deep white matter; dors. = dorsal periventricular; front. = frontal periventricular; post. = posterior periventricular; SHIP = Study of Health in Pomerania; WMH = white matter hyperintensities; WMHC = white matter hyperintensities component.

remained significant (data available from Dryad, table e-5, doi.org/10.5061/dryad.k6k42cq).

We investigated relationships with AD polygenic risk in SHIP participants with available genotyping (n = 985) and found significant cross-sectional association with only WMHC-dors. for participants older than 65 years of age (n = 189, table 4).

Finally, we investigated whether WMHCs were associated with cognitive decline in the BLSA sample (n = 307 and 747 observations; data available from Dryad, table e-6, doi.org/10.5061/dryad.k6k42cq). Only Trail Making Test, Part B was associated with WMHC-dors. We found no associations between any WMHC and Trail Making Test, Part A, Benton Visual Retention Test performance, or California Verbal and Learning Memory Test. Exclusion of participants with mild cognitive impairment (n = 1 and 14 observations) led to similar results (data available from Dryad, table e-7).

Discussion

The current study expands on previous studies that have used total WMH measures by investigating spatial heterogeneity of WMH in large aging cohorts. We identified spatially heterogeneous components of WMH and demonstrated that these components displayed differential associations with age, risk of neurodegeneration, and vascular risk factors. Of note,

WMHC-fron. was evident about 2 decades earlier than the remaining components. WMHC-fron. also showed stronger association with blood pressure and cortical atrophy. Only WMHC-dors. showed associations with AD genetic risk and with longitudinal cognitive decline. The observed spatial heterogeneity is potentially related, in part, to underlying normal heterogeneity in brain anatomy and physiology, as well as heterogeneity of pathophysiologic processes that drive the appearance of these WMH and may have different implications for cognitive outcomes.

WMH have been commonly subdivided into deep and periventricular WMH subclasses.^{27,28} However, the definition of these subdivisions has been inconsistent with a generally poor overlap in WMH subclass ratings.²⁹ It has been suggested that shape provides complementary information for distinguishing WMH subcomponents.³⁰ Another suggestion was to use a simple “distance from the ventricles” measure for the classification into deep and periventricular WMH, but the definition of this distance was variable, arbitrary, and without consensus.^{6,31} Capitalizing on a large sample from the general population and a data-driven method, we systematically categorized WMH without use of prior arbitrary knowledge for defining regional boundaries; rather, those boundaries were detected through clusters of high covariation of WMH occurrence across individuals.

Our data-driven approach separated the deep WMH from the periventricular ones (WMHC-deep vs others) in agreement

Table 4 Associations between WMHCs and risk factors for the cross-sectional SHIP sample

	WMHC-post		WMHC-fron.		WMHC-dors.		WMHC-deep	
	Estimate (SE)	p Value (Bonferroni-corrected)	Estimate (SE)	p Value (Bonferroni-corrected)	Estimate (SE)	p Value (Bonferroni-corrected)	Estimate (SE)	p Value (Bonferroni-corrected)
Vascular and lifestyle risk factors in SHIP^c (n = 1,836, age 22–84 y)								
Sex, female	−0.089 (0.072)	0.860	0.157 (0.061)	0.040 ^a	−0.041 (0.055)	1.000	0.062 (0.050)	0.860
Systolic blood pressure, mm Hg	0.003 (0.002)	0.808	0.006 (0.002)	0.001 ^a	0.003 (0.002)	0.228	0.003 (0.001)	0.116
Intima-media thickness,^b mm	0.294 (0.150)	0.204	0.190 (0.129)	1.000	0.340 (0.117)	0.016 ^a	0.209 (0.104)	0.180
Cigarette smoking								
Ex-smoker	0.244 (0.067)	0.001 ^a	0.054 (0.057)	1.000	0.157 (0.052)	0.008 ^a	0.129 (0.046)	0.020 ^a
Current smoker	0.208 (0.078)	0.032 ^a	0.131 (0.067)	0.204	0.115 (0.060)	0.228	0.128 (0.054)	0.072
Physical activity								
No	0.060 (0.079)	1.000	0.094 (0.068)	1.000	0.056 (0.061)	1.000	0.031 (0.055)	1.000
0–1 h	0.077 (0.093)	1.000	0.024 (0.080)	1.000	0.025 (0.072)	1.000	−0.005 (0.064)	1.000
1–2 h	−0.013 (0.079)	1.000	0.037 (0.067)	1.000	−0.011 (0.061)	1.000	−0.028 (0.054)	1.000
Antihypertensive drugs	0.118 (0.074)	0.440	0.125 (0.063)	0.196	0.075 (0.057)	1.000	0.076 (0.051)	0.544
Lipid-lowering drugs	0.158 (0.109)	0.600	0.079 (0.094)	1.000	0.107 (0.085)	1.000	0.156 (0.076)	0.160
Glycated hemoglobin (HbA_{1c}), %	0.007 (0.047)	1.000	0.003 (0.041)	1.000	0.019 (0.036)	1.000	−0.014 (0.033)	1.000
Waist circumference, cm	0.001 (0.003)	1.000	−0.001 (0.003)	1.000	−0.001 (0.002)	1.000	0.002 (0.002)	1.000
Cholesterol ratio	0.128 (0.153)	1.000	−0.045 (0.132)	1.000	0.079 (0.119)	1.000	0.072 (0.106)	1.000
Antidiabetic drugs	−0.110 (0.175)	1.000	0.166 (0.151)	1.000	0.057 (0.136)	1.000	0.009 (0.122)	1.000
AD genetics in SHIP^c (n = 985, age 22–84 y)								
Polygenic risk score	0.168 (0.114)	0.560	0.101 (0.104)	1.000	0.219 (0.089)	0.056	0.053 (0.078)	1.000

Continued

Table 4 Associations between WMHCs and risk factors for the cross-sectional SHIP sample (continued)

	WMHC-post		WMHC-fron.		WMHC-dors.		WMHC-deep	
	Estimate (SE)	p Value (Bonferroni-corrected)	Estimate (SE)	p Value (Bonferroni-corrected)	Estimate (SE)	p Value (Bonferroni-corrected)	Estimate (SE)	p Value (Bonferroni-corrected)
AD genetics in SHIP^d (n = 189, age >65 y)								
Polygenic risk score	0.798 (0.386)	0.164	0.235 (0.327)	1.000	0.888 (0.326)	0.028 ^a	0.307 (0.257)	1.000

Abbreviations: deep = deep white matter; dors. = dorsal periventricular; fron. = frontal periventricular; post. = posterior periventricular; SHIP = Study of Health in Pomerania; WMHC = white matter hyperintensities component. A linear regression model was used independently for each WMHC using all vascular and lifestyle risk factors jointly as predictors and the WMHC values as the outcome. Similar models were built for the Alzheimer disease polygenic risk score.

^a Significance at level $p < 0.05$.

^b Measure was available for 1,817 participants.

^c Models were adjusted for age, age², education, and SHIP subcohorts.

^d Models were adjusted for age, sex, education, and SHIP subcohorts.

with suggestions in the literature. Of note, the periventricular WMH were also partitioned into posterior and frontal components (WMHC-post. and WMHC-fron.), as well as a more dorsal component (WMHC-dors.). Therefore, we found higher variation in periventricular WMH compared to the deep WMH, a finding not reported in the literature before.

With the nonnegative matrix factorization approach, we assume that the WMH occurrence can be decomposed into highly nonoverlapping parts, where each part groups elements that change in a coordinated fashion across the population. As typical for all factorization methods, it is important to specify the number of components to be extracted. This is the only decision that we have imposed. We determined this number by rigorously examining the coverage of total WMH load and by choosing the largest coverage (data available from Dryad, section e-6, doi.org/10.5061/dryad.k6k42cq). Assessment of the robustness of the final components through reproducibility experiments, using random half-splits of the SHIP sample, showed that the covariance approach would perform consistently in similar populations. The components derived from the BLSA baseline sample (n = 307) were reproducible to a lesser extent, with 66% overlap between components derived from SHIP vs BLSA (data available from Dryad, table e-2). The highest overlap was obtained for the frontal component (91%), maybe because of the existence of similar factors deriving its appearance in both cohorts. However, differences in population characteristics between SHIP and BLSA such as mean age or education and other deriving factors would yield modest overlap in other components.

We observed differential cross-sectional trend lines and longitudinal trajectories, with statistically significant pairwise differences between components, supported by permutation tests. Of note, WMHC-fron. appeared at an earlier age (significant from the fifth decade of life [table 3]) compared to the other components (significant from the sixth decade of life). Prefrontal white matter is most susceptible to the influence of age,³² which might explain why WMHC-fron. was present at earlier age. WMHC-fron. also had a less exponential growth or acceleration with age compared to WMHC-post. and WMHC-dors.; perhaps this result can be reflected with stronger associations between posterior WMH with neurodegenerative processes that tend to accelerate later in life. Although some insights can be taken from our findings regarding AD polygenic risk score and cognition, unfortunately our data cannot provide causal evidence for this result, and further studies are required.

Our results showed that the data-driven components are representing staging as well as different etiologies in WMH appearance. These results are largely expected. The fact that these components were derived from SHIP, which is sampled from the general population with a wide age range (22–84 years), hints to the heterogeneous nature of WMH. Previous research has shown involvement of inflammatory, vascular,

and neurodegenerative diseases in the appearance of WMH. Such conditions are expected to contribute to WMH volume in our sample, according to their prevalence in the general population from the region.

To our knowledge, only one study showed any differential association between regional WMH volume and gray matter atrophy.³³ An interesting finding of our analysis was that the WMHC-fron. component displayed considerably more widespread associations with cortical thinning, in particular in AD-related regions such as the anterior temporal lobe, compared to the other 3 components, especially WMHC-deep and WMHC-post. (figure 1). One explanation could be that WMHC-fron. appeared earlier in life and also showed strong association with blood pressure (tables 3 and 4). It has been demonstrated that frontal WMH were more likely to be present in patients with poststroke vascular dementia compared to healthy controls, and the frontal white matter was more affected than the temporal white matter.³⁴ Our finding of early association of WMHC-fron. with age, increased blood pressure, and more pronounced atrophy is further suggestive of the importance of frontal WMH with respect to neurodegeneration and possibly vascular cognitive dysfunction. Further research is needed to determine whether the WMHC-fron. differentially predicts future vascular dementia.

The posterior periventricular, dorsal, and deep white matter components were associated with smoking. The mechanisms for the association between smoking and posterior periventricular WMH and deep WMH can be potentially explained by different nicotine receptor distribution in the brain.³⁵ The link between intima-media thickness and WMH may primarily reflect shared risk factors such as smoking.³⁶ While associations between these risk factors and regional WMH have been reported previously,^{37,38} a contribution of our analysis lies in the application of a data-driven method, which “categorizes” those changes across the population together. Few MRI studies have such statistical power, with a population-based sample and a very high standardization protocol.

A recent study showed that WMH volume is significantly elevated among individuals with autosomal dominant genetic mutations for AD. These changes are most pronounced in posterior periventricular regions.³⁹ In our study, only the periventricular dorsal component showed a significant association with the AD polygenic risk score in individuals older than 65 years that survived Bonferroni correction (table 4). Because the prevalence of sporadic AD increases rapidly after the age of 65, our findings might reflect a contribution of AD pathology to the development of WMH.

A very striking result in our analysis was that WMH-dors., which showed a significant association with the AD polygenic risk score after the age of 65 years, was also significantly associated with longitudinal cognitive decline in the validation sample BLSA. This finding is further suggestive of a potential

role of impairment in cognitive abilities and dementia-related degeneration with focal appearance of WMH in periventricular dorsal regions.

Studies utilizing advanced structural covariance analysis for systematically investigating spatial heterogeneity of WMH are rare. A few recent studies used a similar methodology for examining regional structural covariance in aging populations.¹⁶ However, these studies were limited to analysis of gray matter. Another strength of our work is the rich cohorts included. The large population-based sample in SHIP, which spans a wide age range, allowed us to reliably define WMH patterns and to study their correlates. The BLSA cohort provided a valuable longitudinal sample to examine trajectories of WMHCs.

Despite the above strengths, certain limitations should be noted. First, some modifiable risk factors, such as dietary factors (e.g., salt or sugar intake) and inflammation, were not included in the study. Second, our analysis did not include periventricular spaces, or further small vessel disease subtype assessment, and those should be considered in future research. Third, although associations between WMHCs and risk factors or AD polygenic risk score are suggestive and reasonable, such correlational analyses do not establish causality and are potentially limited by the high correlation between the components and total WMH volume (data available from Dryad, table e-8 and figure e-5, doi.org/10.5061/dryad.k6k42cq). Fourth, The SHIP participants did not have complete cognitive testing. Therefore, some brain changes in the SHIP sample are more specific to aging, but also others might be driven by unrecognized changes and that might represent the initial impairment in people with vascular cognitive disorder. Fifth, several of the findings were not robust to exclusion of relatively few participants with (possible) cognitive impairment; as a result, a small proportion of participants may be primarily deriving some of the observed associations. Sixth, our strict quality control criteria resulted in a high number of scans excluded in SHIP, which might lead to potential bias and less generalizability of our results. Finally, The BLSA sample with available T1 and fluid-attenuated inversion recovery scans that we used for studying longitudinal associations was rather small. Repeated assessments continue in BLSA, and future studies should consider larger samples with longer follow-up intervals.

Our study indicates that WMH appearance follows systematic and co-occurring regional patterns. We found an early involvement of the periventricular frontal regions, with strong associations with blood pressure and more pronounced cortical atrophy through the adult lifespan. The periventricular dorsal component showed associations with AD polygenic risk score and cognitive decline, as well as later appearance in the aging brain. Our findings support the hypothesis that the appearance of WMH follows age- and disease-dependent regional distribution patterns, potentially influenced by differential underlying pathophysiologic mechanisms, and possibly

with different implications for vascular risk factors as well as neurodegenerative and cognitive outcomes.

Author contributions

M.H.: drafting the manuscript for content, including medical writing for content, study concept or design, analysis or interpretation of data, acquisition of data, statistical analysis, study supervision or coordination, obtaining funding, and final approval. A.S.: analysis or interpretation of data, and final approval. G.E.: analysis or interpretation of data, and final approval. J.T.: analysis or interpretation of data, and final approval. D.J.: analysis or interpretation of data, and final approval. D.A.W.: analysis or interpretation of data, and final approval. H.S.: analysis or interpretation of data, study concept or design, and final approval. N.B.: analysis or interpretation of data, and final approval. J.D.: analysis or interpretation of data, and final approval. H.V.: analysis or interpretation of data, and final approval. U.S.: analysis or interpretation of data, and final approval. W.H.: study concept or design, analysis or interpretation of data, and final approval. S.M.R., H.J.G., and C.D.: drafting the manuscript for content, including medical writing for content, study concept or design, analysis or interpretation of data, study supervision or coordination, obtaining funding, and final approval.

Study funding

SHIP is part of the Community Medicine Research net of the University of Greifswald, Germany, which is funded by the Federal Ministry of Education and Research (grants 01ZZ9603, 01ZZ0103, and 01ZZ0403), the Ministry of Cultural Affairs, and the Social Ministry of the Federal State of Mecklenburg-West Pomerania. Genome-wide data in SHIP and MRI scans in SHIP and SHIP-TREND have been supported by a joint grant from Siemens Healthineers, Erlangen, Germany, and the Federal State of Mecklenburg-West Pomerania. Genome-wide genotyping in SHIP-TREND-0 was supported by the Federal Ministry of Education and Research (grant 03ZIK012). This work was supported in part by NIH grants R01-AG14971 and R01 AG054409. J.B. Toledo was supported by P01 AG032953, PO1 AG017586, P30 AG010124, and P50 NS053488. This work was supported in part by the Intramural Research Program, National Institute on Aging, NIH. Dr. Mohamad Habes was supported in part by the Alfried Krupp von Bohlen und Halbach Foundation. No conflict of interest to be declared. This work has been supported in part by the Allen H. and Selma W. Berkman Charitable Trust (Accelerating Research on Vascular Dementia) and NIH (grant 1RF1AG054409).

Disclosure

The authors report no disclosures relevant to the manuscript. Go to Neurology.org/N for full disclosures.

Received July 28, 2017. Accepted in final form June 4, 2018.

References

1. Wardlaw JM, Smith C, Dichgans M. Mechanisms of sporadic cerebral small vessel disease: insights from neuroimaging. *Lancet Neurol* 2013;12:483–497.

- Appel J, Potter E, Bhatia N, et al. Association of white matter hyperintensity measurements on brain MR imaging with cognitive status, medial temporal atrophy, and cardiovascular risk factors. *AJNR Am J Neuroradiol* 2009;30:1870–1876.
- Habes M, Erus G, Toledo JB, et al. White matter hyperintensities and imaging patterns of brain aging in the general population. *Brain* 2016;139(pt 4):1164–1179.
- Prins ND, Scheltens P. White matter hyperintensities, cognitive impairment and dementia: an update. *Nat Rev Neurol* 2015;11:157–165.
- Young VG, Halliday GM, Kril JJ. Neuropathologic correlates of white matter hyperintensities. *Neurology* 2008;71:804–811.
- Kim KW, MacFall JR, Payne ME. Classification of white matter lesions on magnetic resonance imaging in elderly persons. *Biol Psychiatry* 2008;64:273–280.
- Polvikoski TM, van Straaten ECW, Barkhof F, et al. Frontal lobe white matter hyperintensities and neurofibrillary pathology in the oldest old. *Neurology* 2010;75:2071–2078.
- Simpson JE, Ince PG, Higham CE, et al. Microglial activation in white matter lesions and nonlesional white matter of ageing brains. *Neuropathol Appl Neurobiol* 2007;33:670–683.
- Fernando MS, Simpson JE, Matthews F, et al. White matter lesions in an unselected cohort of the elderly: molecular pathology suggests origin from chronic hypoperfusion injury. *Stroke J Cereb Circ* 2006;37:1391–1398.
- de Leeuw FE, de Groot JC, Bots ML, et al. Carotid atherosclerosis and cerebral white matter lesions in a population based magnetic resonance imaging study. *J Neurol* 2000;247:291–296.
- Marnane M, Al-Jawadi OO, Mortazavi S, et al. Periventricular hyperintensities are associated with elevated cerebral amyloid. *Neurology* 2016;86:535–543.
- van Straaten ECW, Harvey D, Scheltens P, et al. Periventricular white matter hyperintensities increase the likelihood of progression from amnesic mild cognitive impairment to dementia. *J Neurol* 2008;255:1302–1308.
- Kim S, Choi SH, Lee YM, et al. Periventricular white matter hyperintensities and the risk of dementia: a CREDOS study. *Int Psychogeriatr* 2015;27:2069–2077.
- Smith CD, Johnson ES, Van Eldik LJ, et al. Peripheral (deep) but not periventricular MRI white matter hyperintensities are increased in clinical vascular dementia compared to Alzheimer's disease. *Brain Behav* 2016;6:e00438.
- Debette S, Bombois S, Bruandet A, et al. Subcortical hyperintensities are associated with cognitive decline in patients with mild cognitive impairment. *Stroke J Cereb Circ* 2007;38:2924–2930.
- Alexander-Bloch A, Giedd JN, Bullmore E. Imaging structural co-variance between human brain regions. *Nat Rev Neurosci* 2013;14:322–336.
- Sotiras A, Resnick SM, Davatzikos C. Finding imaging patterns of structural covariance via non-negative matrix factorization. *Neuroimage* 2015;108:1–16.
- Sotiras A, Toledo JB, Gur RE, Gur RC, Satterthwaite TD, Davatzikos C. Patterns of coordinated cortical remodeling during adolescence and their associations with functional specialization and evolutionary expansion. *Proc Natl Acad Sci USA* 2017;114:3527–3532.
- Völzke H, Alte D, Schmidt CO, et al. Cohort profile: the study of health in Pomerania. *Int J Epidemiol* 2011;40:294–307.
- Habes M, Janowitz D, Erus G, et al. Advanced brain aging: relationship with epidemiologic and genetic risk factors, and overlap with Alzheimer disease atrophy patterns. *Transl Psychiatry* 2016;6:e775.
- Resnick SM, Goldszal AF, Davatzikos C, et al. One-year age changes in MRI brain volumes in older adults. *Cereb Cortex* 2000;10:464–472.
- Hegenscheid K, Kühn JP, Völzke H, Biffar R, Hosten N, Puls R. Whole-body magnetic resonance imaging of healthy volunteers: pilot study results from the population-based SHIP study. *Rofo* 2009;181:748–759.
- Venkatraman VK, Gonzalez CE, Landman B, et al. Region of interest correction factors improve reliability of diffusion imaging measures within and across scanners and field strengths. *Neuroimage* 2015;119:406–416.
- Grothe MJ, Barthel H, Sepulcre J, Dyrbal M, Sabri O, Teipel SJ. In vivo staging of regional amyloid deposition. *Neurology* 2017;89:2031–2038.
- Habes M, Toledo JB, Resnick SM, et al. Relationship between APOE genotype and structural MRI measures throughout adulthood in the study of health in Pomerania population-based cohort. *AJNR Am J Neuroradiol* 2016;37:1636–1642.
- R Development Core Team. R: A Language and Environment for Statistical Computing. Vienna: R Foundation for Statistical Computing; 2008. Available at: R-project.org. Accessed January 1, 2016.
- Scheltens P, Barkhof F, Leys D, et al. A semiquantitative rating scale for the assessment of signal hyperintensities on magnetic resonance imaging. *J Neurol Sci* 1993;114:7–12.
- Fazekas F, Chawluk JB, Alavi A, Hurtig HI, Zimmerman RA. MR signal abnormalities at 1.5 T in Alzheimer's dementia and normal aging. *AJR Am J Roentgenol* 1987;149:351–356.
- Mantyla R, Erkinjuntti T, Salonen O, et al. Variable agreement between visual rating scales for white matter hyperintensities on MRI: comparison of 13 rating scales in a poststroke cohort. *Stroke J Cereb Circ* 1997;28:1614–1623.
- Schmidt R, Schmidt H, Haybaeck J, et al. Heterogeneity in age-related white matter changes. *Acta Neuropathol* 2011;122:171–185.
- DeCarli C, Fletcher E, Ramey V, Harvey D, Jagust WJ. Anatomical mapping of white matter hyperintensities (WMH): exploring the relationships between periventricular WMH, deep WMH, and total WMH. *Burden Stroke* 2005;36:50–55.
- Gunning-Dixon FM, Brickman AM, Cheng JC, Alexopoulos GS. Aging of cerebral white matter: a review of MRI findings. *Int J Geriatr Psychiatry* 2009;24:109–117.

33. Wen W, Sachdev PS, Chen X, Anstey K. Gray matter reduction is correlated with white matter hyperintensity volume: a voxel-based morphometric study in a large epidemiological sample. *Neuroimage* 2006;29:1031–1039.
34. Chen A, Akinyemi RO, Hase Y, et al. Frontal white matter hyperintensities, clasmato-dendrosis and gliovascular abnormalities in ageing and post-stroke dementia. *Brain J Neurol* 2016;139(pt 1):242–258.
35. Zoli M, Pistillo F, Gotti C. Diversity of native nicotinic receptor subtypes in mam-malian brain. *Neuropharmacology* 2015;96(pt B):302–311.
36. Polak JF, Pencina MJ, Meisner A, et al. Associations of carotid artery intima-media thickness (IMT) with risk factors and prevalent cardiovascular disease: comparison of mean common carotid artery IMT with maximum internal carotid artery IMT. *J Ultrasound Med* 2010;29:1759–1768.
37. Fukuda H, Kitani M. Cigarette smoking is correlated with the periventricular hyperintensity grade of brain magnetic resonance imaging. *Stroke J Cereb Circ* 1996;27:645–649.
38. van Dijk EJ, Breteler MMB, Schmidt R, et al. The association between blood pressure, hypertension, and cerebral white matter lesions: cardiovascular determinants of de-mentia study. *Hypertension* 2004;44:625–630.
39. Lee S, Viqar F, Zimmerman ME, et al. White matter hyperintensities are a core feature of Alzheimer's disease: evidence from the dominantly inherited Alzheimer network. *Ann Neurol* 2016;79:929–939.